Ionic Charge Effects on the Sedimentation Rate and Intrinsic Viscosity of Polyelectrolytes. T7 DNA

Dirk Stigter

Department of Materials Science and Mineral Engineering, University of California, Berkeley, California 94720. *Received December 20, 1984*

ABSTRACT: This paper discusses the large changes of the sedimentation coefficient, s^0, and the intrinsic viscosity, $[\eta]$, of polyelectrolytes upon variation of the foreign salt concentration, in particular in T7 DNA–NaCl solutions. The analysis is based on the model of a wormlike chain, surrounded by a Gouy–Chapman ionic double layer, and rests on the following theories: transport properties of uncharged polymers by Yamakawa and Fujii (1973, 1974) and Monte Carlo computations by Zimm (1980); the electric persistence length by Le Bret (1981) and by Fixman (1982); the excluded volume effect in coil swelling by Stigter (1982); and the ionic relaxation effect on the sedimentation of charged rods by Stigter (1982). Extensions of the theory are as follows: triple interactions between chain segments in the excluded volume theory; incorporation of the short-range relaxation effect in s^0 and in $[\eta]$ by renormalizing the hydrodynamic diameter of the chain; and linking the long-range electric field effect of the relaxation dipoles to the electrophoretic mobility of the polyelectrolyte for the *approximate* model of a uniformly polarizable polyelectrolyte sphere with complete drainage. The experimentally observed dependence of s^0 and of $[\eta]$ on ionic strength is well explained by the theory and is mainly caused by the electrostatic coil expansion. The comparison between theory and experiment yields two independent estimates of the intrinsic persistence length, P_0, of native T7 DNA: $P_0 \approx 350$ Å from s^0 and $P_0 \approx 425$ Å from $[\eta]$. A large discrepancy is reported between two theories of the ionic relaxation effect of a sedimenting or diffusing polyelectrolyte sphere. A small relaxation effect is predicted by the electrohydrodynamic theory of Booth (1954), while a very large relaxation effect is derived by Schurr using fluctuation theory (1980). The experiments on T7 DNA agree with Booth's approach used in the present analysis.

1. Introduction

Among the most striking observations on polyelectrolyte–salt solutions is the large influence of the salt concentration on the transport properties. This is well illustrated by the sedimentation and viscosity experiments on T7 DNA by Rosenberg and Studier[1] and by Rinehart and Hearst.[2] This paper is concerned with the interpretation of the limiting sedimentation coefficient, s^0, and the intrinsic viscosity, $[\eta]$, of polyelectrolytes, in particular of T7 DNA.

The molar friction factor f_p of single polyelectrolyte molecules, proportional to $1/s^0$, can also be obtained from the diffusion coefficient by the Einstein relation $D^0 = RT/f_p$. In recent years diffusion measurements by dynamic light scattering have largely replaced friction determinations by ultracentrifugal sedimentation. As a consequence, there is renewed interest in salt effects on the friction of charged macromolecules.

Although known since the beginning of polyelectrolyte research, the charge effects on $[\eta]$ and on f_p have never been treated in a satisfactory way, partly because of a lack of good experimental data on well-defined systems and partly because the theoretical models and assumptions were not good enough. Qualitatively, the charge effects on the transport properties of isolated polyelectrolyte coils have been explained in two different ways. First, the flow component perpendicular to the chain causes a local asymmetry of the double layer, due to the finite mobility of the small ions. This so-called relaxation effect increases the friction of the chain in sedimentation as well as in viscosity experiments. The second explanation is based on the electrostatic coil expansion due to the mutual repulsion of the fixed charges. Just as for uncharged polymers, a size increase of polyelectrolyte coils gives rise to larger values of the intrinsic viscosity and of the friction factor.

In recent years good progress has been made on various aspects of the theory. We shall use results by Yamakawa and Fujii[3,4] and by Zimm,[5] who have studied the hydrodynamics of uncharged linear polymers as a function of chain length. The relaxation effect on the translational friction has been treated for two different models, by Schurr[6] for a uniformly charged, permeable sphere and by Stigter[7] for a charged rod in transverse motion. The electrostatic persistence length has been treated by Le Bret[8] and by Fixman[9] for wormlike chains with a Gouy–Chapman electrical double layer. For the same model Stigter[10] has derived the excluded volume effect, using pair interactions between charged chain segments. In this paper the various theories, and suitable extensions, are combined in a test of the data for T7 DNA. From sequencing studies Dunn and Studier[11b] have found 39 936 base pairs per T7 DNA molecule with a molecular weight 26.43×10^6. We shall use these results in the computations, with a rise of 3.37 Å per base pair. Several theoretical models of polyelectrolytes have been presented in the literature, the main ones being the permeable sphere and the charged, wormlike chain. The latter model is closest to an actual polyelectrolyte chain and is used in the present treatment. Under equilibrium conditions one assumes a Gouy–Chapman ionic atmosphere with cylinder symmetry around short segments of the chain, as pictured in Figure 1.

The paper is organized in several parts. Section 2 begins with a review of coil swelling. A novel aspect is the introduction of triple interactions between chain segments in the excluded volume theory.

The available theory of the ionic relaxation effect also needs some extensions. For polyelectrolytes it has two parts. The short-range part, in section 3, concerns the modification of the fluid flow around a single chain segment, augmenting the friction of the segment and represented as an increase of the hydrodynamic diameter of the chain. The increased chain diameter is a convenient way to introduce the relaxation effect also in viscosity theory. The second, long-range part of the relaxation effect, typical for polyelectrolyte coils and treated in sections 4 and 5, arises from the electric dipole field around each moving chain segment and its lagging ionic atmosphere. Each segment finds itself in the resultant electric field of all other dipolar segments; the reduction in the relative velocity of the segment is proportional to the electrophoretic velocity of the chain. The total effect is akin to that of the sedimentation potential in a concentrated polyelec-

0024-9297/85/2218-1619$01.50/0

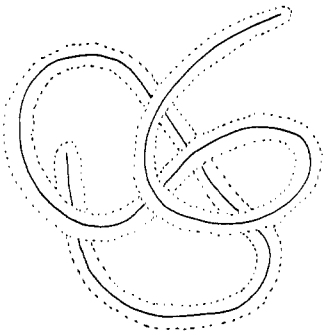

Figure 1. Polyelectrolyte model with Gouy–Chapman ionic double layer under static conditions.

trolyte solution, the basis of our treatment. The effects of the dipole potentials cancel in viscosity, at least in a first approximation.

The Yamakawa–Fujii theories[3,4] for uncharged wormlike chains without excluded volume are used for the hydrodynamic interaction between the segments in sedimentation, section 4, and in viscosity, section 5. In both cases the preaveraging approximations employed in the interaction theories[3,4] are corrected on the basis of Zimm's results of Monte Carlo computations.[5] The statistics of DNA coils is modified to eliminate the excluded volume effect, prior to application of the hydrodynamic theory.[3-5]

2. Coil Swelling

We consider an isolated polyelectrolyte coil in a salt solution. The repulsion between charges fixed to the chain has two effects on the coil statistics. In the first place, the repulsion between vicinal charges along a chain segment stiffens the chain, leading to an increase of its persistence length, from P_0 for the uncharged polymer to

$$P = P_0 + P_{el} \tag{1}$$

for the charged polyelectrolyte. The electrostatic contribution P_{el} has been evaluated independently by Le Bret[8] and by Fixman[9] for the Gouy–Chapman model of the uniformly charged, flexible rod, essentially by numerical integration of the Poisson–Boltzmann equation around the curved rod. Although their methods are somewhat different, overlapping results agree within computational uncertainties.

For sufficiently long chains, such as T7 DNA, there is also an excluded volume effect, due to the electrostatic repulsion between remotely connected chain segments. This interaction between segment pairs is evaluated[10] in terms of the osmotic pressure second virial coefficient B_2 for charged long rods of length l and effective diameter d_B

$$B_2 = (\pi/4)l^2 d_B \tag{2}$$

When the contour length of the chain is L, it is divided into L/l segments which have a concentration ρ in the coil volume V. In analogy with the McMillan–Mayer solution theory, the total free energy F of the interaction between segment pairs is

$$F/kT = B_2 \int_V \rho^2 \, dV \tag{3}$$

The free energy F perturbs the Gaussian probability of finding an end-to-end distance h of the chain between h and $h + dh$

$$W(h)\, dh = \text{constant} \times h^2 \exp(-3h^2/4LP - F/kT)\, dh \tag{4}$$

The mean square of h is

$$\langle h^2 \rangle = \int_0^\infty h^2 W(h)\, dh \Big/ \int_0^\infty W(h)\, dh \tag{5a}$$

Following the Hermans–Overbeek approximation[11a] we take the value that maximizes the function $hW(h)$:

$$\frac{\partial}{\partial h}\{h^3 \exp(-3h^2/4LP - F/kT)\} = 0 \qquad \text{at } h^2 = \langle h^2 \rangle \tag{5b}$$

A measure of the coil size is its mean square radius of gyration, given by

$$s^2 = (\langle h^2 \rangle + 2LP)/12 \tag{6}$$

In the absence of excluded volume effects, $F = 0$, eq 5 and 6 give the results of random flight statistics for long chains: $\langle h^2 \rangle = 2LP$ and $s^2 = LP/3$.

The exact segment distribution ρ in polyelectrolyte coils is not known, but we can adopt an approximation for ρ. With eq 2–6 this is sufficient to derive an equation of the form

$$G(L,P,s) = d_B \tag{7}$$

In eq 7 the contour length L of the polyelectrolyte is constant and the persistence length P and the effective chain diameter d_B can be evaluated as a function of the ionic strength.[8,9,12] With such information eq 7 can be solved for the radius of gyration s, thus giving the coil size as a function of ionic strength.

The function $G(L,P,s)$ is available for three approximate distributions ρ. In the simplest model the segments are distributed uniformly over a spherical volume. For this uniform sphere eq 7 becomes[10]

$$\frac{137.7s^5(3s^2 - LP)}{L^3P(6s^2 - LP)} = d_B \tag{8a}$$

The result for the random flight coil[10,13] differs from eq 8a only by a numerical factor $4/\pi$

$$\frac{175.3s^5(3s^2 - LP)}{L^3P(6s^2 - LP)} = d_B \tag{8b}$$

The uniformly filled ellipsoidal coil model[14] yields[10]

$$\frac{4.417(9s^2 - LP)^{3/2}(3s^2 - LP)}{L^2(6s^2 - LP)} = d_B \tag{8c}$$

Table I gives information on the various coil parameters for T7 DNA in NaCl solutions. The values of d_B were obtained for a transport model of duplex DNA: a rod with a diameter of 24 Å, a charge of 0.65 electron per phosphate group, and a Gouy–Chapman ionic atmosphere.[12,15] The rod model for P_{el} used by Fixman[9] has a diameter of 20 Å and a Gouy–Chapman double layer with the full phosphate charge. Results for the radius of gyration s are given for the three coil density models in eq 8, using an intrinsic persistence length $P_0 = 400$ Å. The differences between the three models for ρ are minor, maximal 3%. It is clear that the excluded volume effect is not very sensitive to the details of the coil model.

Without excluded volume effect the mean square radius of gyration would be $s^2 = LP/3$, consistent with eq 8 for $d_B = 0$. Following Flory[16,17] one may express the excluded volume effect in terms of an expansion factor α, defined by

$$\alpha^2 = 3s^2/LP \tag{9}$$

Table I shows values of the relative volume increase, α^3, for the uniform spherical coil of eq 8a. It is interesting that for T7 DNA the excluded volume effect may cause a nearly

Table I
Expansion of T7 DNA in Aqueous Sodium Chloride Solutions at 25 °C

M_{NaCl}	d_B,[a] Å	P,[b] Å	radius of gyration s, Å			α^{3c}	Δ^d
			eq 8a	eq 8b	eq 8c		
1.0	29.7	461	4807	4756	4741	1.181	6.21×10^{-5}
0.5	34.1	470	4881	4825	4809	1.201	7.82×10^{-5}
0.2	44.1	484	5014	4946	4928	1.246	1.21×10^{-4}
0.1	56	496	5145	5065	5046	1.298	1.80×10^{-4}
0.05	74	511	5315	5219	5201	1.368	2.85×10^{-4}
0.02	112	536	5613	5490	5477	1.500	5.55×10^{-4}
0.01	157	568	5903	5783	5782	1.599	9.37×10^{-4}
0.005	224	614	6335	6163	6180	1.759	1.54×10^{-3}
0.002	363	731	7109	6899	6947	1.913	2.87×10^{-3}
0.001	529	887	7919	7679	7748	1.978	4.41×10^{-3}

[a] Effective diameter of DNA cylinder for pair interaction.[12] [b] Total persistence length $P = P_0 + P_{el}$ with $P_0 = 400$ Å and P_{el} according to Fixman.[9] [c] Coil expansion due to excluded volume. [d] Correction term for triplet segment interactions, eq 16.

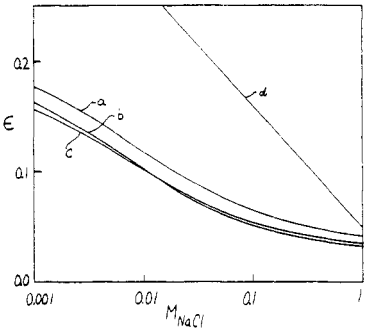

Figure 2. Excluded volume exponent ϵ in eq 10 vs. ionic strength for different coil models of T7 DNA. Curve a, uniform sphere; curve b, Gaussian sphere; curve c, uniform ellipsoidal coil; curve d, empirical relation by Douthart and Bloomfield[19] for total charge effect on coil size.

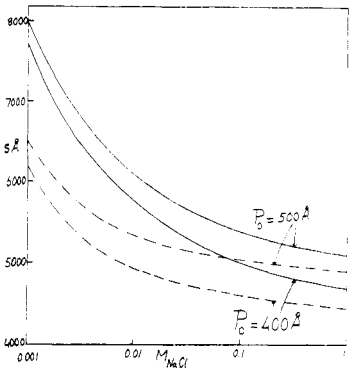

Figure 3. Radius of gyration s of coiled T7 DNA in NaCl solutions from uniform spherical model for excluded volume, eq 8a, with values of intrinsic persistence length P_0 as indicated. Dashed curves from eq 8a with $d_B = 0$, no excluded volume.

twofold increase of the coil volume.

Another way of expressing excluded volume effects is that by Peterlin[18] in terms of a fractional exponent ϵ. In the present notation we have

$$\langle h^2 \rangle = (2P)^2(L/2P)^{1+\epsilon} \tag{10a}$$

For given values of s, L, and P eq 6 and 10a yield

$$\epsilon = \ln\left(\frac{6s^2}{LP} - 1\right) \Big/ \ln\left(\frac{L}{2P}\right) \tag{10b}$$

For $\epsilon = 0$ the results of random flight coils are recovered from eq 10, $\langle h^2 \rangle = 2LP$ and $s^2 = LP/3$. Curves of ϵ vs. M_{NaCl} for T7 DNA are shown in Figure 2 for the three coil models under study, assuming an intrinsic persistence length $P_0 = 400$ Å. The difference between the models is not large. Our values of ϵ fall far below the straight line representing the empirical relation $\epsilon = 0.05 - 0.11 \log M_{NaCl}$ reported by Douthart and Bloomfield[19] for linear DNA. The large difference is not surprising since the empirical relation includes not only the excluded volume effect but also the charge effect on the persistence length. The comparison in Figure 2 indicates that for T7 DNA these two contributions to coil expansion are of the same order of magnitude.

In Figure 3 the radius of gyration, s, derived with the uniformly filled spherical coil model of eq 8a, is plotted vs. the ionic strength, taking $P_0 = 400$ and 500 Å. As expected, stiffening of the chain increases the coil size. The dashed curves, computed with $d_B = 0$ in eq 8a, or $s^2 = LP/3$, show the salt effects on the persistence length only. The fairly large excluded volume effects in Figure 3, based on segment pair interactions, have led us to investigate contributions of triple-segment interactions. The following discussion, however, shows that higher than pair segment interactions do not add significantly to the excluded volume effect.

We return to the development sketched in eq 2–8 for the uniformly filled sphere. For this model the concentration of chain segments of length l is uniform in the coil volume V and equals

$$\rho = L/lV \tag{11}$$

where $V = (4/3)\pi(5/3)^{3/2}s^3$. The triplet-segment interactions are introduced in eq 3 where the total intrachain interaction free energy now is

$$F/kT = V(B_2\rho^2 + B_3\rho^3) \tag{12}$$

As far as we know, the rigorous derivation of the third virial coefficient B_3 for long rods, by integration of the relevant cluster integral, is not available. Therefore, we obtain B_3 from the scaled particle theory.[20] For an isotropic fluid of rods of length l and radius a at a density ρ, the scaled particle theory yields for the pressure[20]

$$\frac{p}{kT} = \frac{1 + B + C + D + (B + C)^2 + (D/3)(B + 3C/2)}{(1 - B - C)^3}\rho \tag{13}$$

where $B = \pi a^2 l\rho$, $C = (4\pi/3)a^3\rho$, and $D = (\pi/2)al^2\rho$. We take the long-rod limit, $l \gg a$, where $C \ll B \ll D$ and eq 13 may be approximated with

$$p/kT = (1 + D + DB/3)\rho = \rho + (\pi/2)al^2\rho^2 + (\pi^2/6)a^3l^3\rho^3 \tag{14}$$

According to the McMillan–Mayer theory the pressure of the one-component fluid of rods is formally the same as the osmotic (or Donnan) pressure of a rodlike solute in a multicomponent solvent. As before, we approximate the

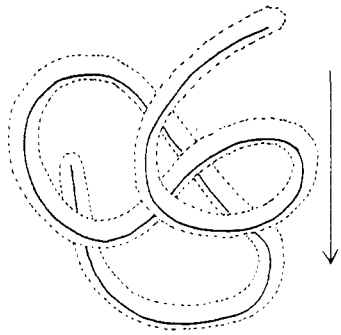

Figure 4. Polyelectrolyte model of Figure 1, sedimenting in the direction of the arrow, with asymmetrically perturbed ionic double layer.

intrachain interactions by the interactions between the unconnected segments in the coil volume. In addition, we set $2a = d_B$ in eq 14. This makes the expression for B_2 exact, as in eq 2; it might introduce an error in B_3, in particular at low ionic strength where the repulsive potential–distance curve is not very steep and the averaging in the cluster integrals for B_2 and B_3 might lead to significantly different effective chain diameters.

With eq 14 the intrachain free energy becomes

$$F/kT = V(\pi d_B l^2 \rho^2/4 + \pi^2 d_B{}^3 l^3 \rho^3/48) = V(\pi d_B L^2/(4V^2) + \pi^2 d_B{}^3 L^3/(48V^3)) \quad (15)$$

We note that with eq 11 the segment length cancels in both terms of eq 15. After some tedious but straightforward algebra the result of eq 4–6 and 15 can be put in the form of eq 8a with a correction term

$$\frac{137.7s^5(3s^2 - LP)}{L^3P(6s^2 - LP)} = d_B(1 + 0.0581Ld_B{}^2/s^3) = d_B(1 + \Delta) \quad (16)$$

Table I presents values of Δ as a function of the salt concentration. The correction corresponds to a negligibly small change of d_B in eq 8a, less than 0.5% in all cases.

3. Relaxation Effect and Renormalization of the Hydrodynamic Chain Diameter

The relaxation effect has recently been treated for the sedimentation of highly charged, colloidal spheres[21] and also for long, straight, highly charged colloidal rods[7] moving sideways in sedimentation. We now apply these results to the sedimentation and to the viscosity of polyelectrolyte coils. Figure 4 shows schematically how the ionic atmosphere is distorted when the coiled chain sediments in the direction of the arrow. The degree of distortion depends on the orientation of the chain segment: no relaxation effect for segments parallel to the direction of motion, maximum asymmetry for perpendicular orientation. We consider only effects which are linear in the applied field and we average for random orientation.

One of the problems is how to introduce the relaxation effect into the intersegmental hydrodynamic interactions. Our approach is based on the fact that the relaxation perturbation and the intersegmental interactions involve different parts of the hydrodynamic flow field. The relaxation modifies the liquid flow only close to the charged cylinder surface, *inside* the electrical double layer. On the other hand, the interactions between segments are longer range and are determined almost exclusively by the flow field *outside* the double layer.

We account for the relaxation effect by an increase of the hydrodynamic diameter of the rod, from d to d_{rel}. In this section we show that this renormalization leaves the flow field outside the double layer unchanged. We consider only an angular average of the liquid velocity, similar to preaveraging the Oseen tensor, a widely used approximation in polymer hydrodynamics.

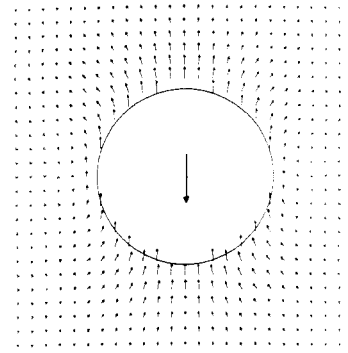

Figure 5. Relaxation part of fluid velocity around a charge sphere, sedimenting in the direction of the large arrow in salt solution with Debye length $1/\kappa = 0.71a$.

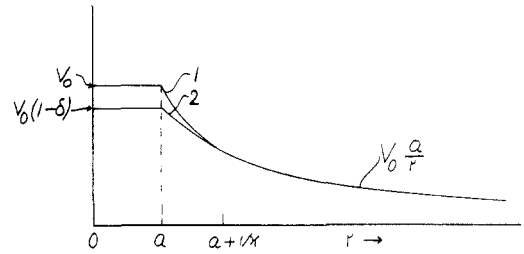

Figure 6. Schematic comparison of average liquid velocity around uncharged sphere, curve 1 from eq 17, and around charged sphere, curve 2.

To develop the procedure we first consider the simple case of a sphere of radius a sedimenting with velocity $v_0 = K/6\pi\eta a$, where K is the sedimentation force on the sphere. The average liquid velocity at distance r from the sphere is by symmetry in the sedimentation direction. If the sphere is uncharged, this angular average, denoted $\langle v_r \rangle$, can be derived from the Stokes field. The well-known result is

$$\langle v_r \rangle = v_0 a/r \quad (17)$$

The interesting case is the flow field around the sphere when it is charged, sedimenting in a salt solution. Now the relaxation effect adds an extra component to the Stokes field. This additional flow[21] is reproduced in Figure 5 as a vector field, in a cross section containing the axis of rotational symmetry around a charged sphere sedimenting in a salt solution with Debye length $1/\kappa = 0.71a$. It is clear that the extra velocity decays much faster than $1/r$ and does not extend beyond the ionic atmosphere.

Figure 6 presents a schematic comparison of $\langle v_r \rangle$ vs. r for the charged and the uncharged sphere. Only the inner flow fields are different. The invariance of the outer flow field follows from the balance of forces on the sphere. The asymmetric ionic atmosphere exerts an extra electric force on the charged sphere which diminishes the sedimentation force K. Furthermore, the extra flow, pictured in Figure 5, exerts an extra hydrodynamic drag force which decreases the total friction on the sphere. A detailed treatment[22] shows that these two extra forces cancel each other. Since the hydrodynamic equations are linear, the relaxation flow field is added to the Stokes field around the uncharged sphere. The velocity of the sphere decreases hereby from v_0 to $v_0(1 - \delta)$.

We now replace the charged sphere of radius a by an uncharged sphere of radius a_{rel} and with the same velocity

Table II
Factors in Eq 42 and 45 for T7 DNA in Aqueous Sodium Chloride Solutions

M_{NaCl}	d_{rel},[a] Å	P_{eff},[b] Å	$3\pi\eta_0 L/f$[c]	$(u/E) \times 10^4$,[d] cm^2 V^{-1} s^{-1}	$1 + \Delta s^0/s^0$ [e]	$\Phi \times 10^{-23}$[f]
1	(24.0)	515				1.575
0.5	(24.4)	531				1.564
0.2	(25.1)	560				1.546
0.1	25.8	590	19.74	3.22	0.998	1.527
0.05	26.9	629	19.20	3.46	0.996	1.505
0.02	28.9	702	18.34	3.83	0.990	1.468
0.01	30.6	783	17.53	4.05	0.979	1.428
0.005	33.1	894	16.61	4.26	0.961	1.380
0.002	37.2	1126	15.17	(4.5)	0.928	1.293
0.001	(42)	1396	13.97	(4.65)	0.867	1.213

[a] Equation 32, values in parentheses by extrapolation. [b] $P_{eff} = 3s^2/L$ with s from Table I, eq 8a, $P_0 = 400$ Å. [c] Equation 37. [d] Reference 30, corrected to 20 °C; values in parentheses by extrapolation. [e] Equation 41. [f] Equation 45.

$v_0(1 - \delta)$. Around this uncharged sphere the average liquid velocity is, following Stokes,

$$\langle v_r \rangle = v_0(1 - \delta)a_{rel}/r \tag{18}$$

The requirement that this field, for large r, be the same as that in eq 17, gives the desired renormalization

$$a_{rel} = a/(1 - \delta) \tag{19}$$

We proceed with the sideways sedimentation of a long rod of diameter d. It is convenient to assume the rod to be at rest, with the liquid flowing past it, with constant velocity at infinite distance from the axis of the rod. For the inner flow field, near the surface and not too close to the ends of the rod, the simple two-dimensional form derived for the infinitely long rod is a good approximation. From the radial and angular components of the liquid velocity, v_r and v_ϑ, we derive the angular average in the direction of sedimentation with

$$\langle v_r \rangle_\perp = \frac{1}{2\pi}\int_0^{2\pi} (v_r \cos\vartheta - v_\vartheta \sin\vartheta)\, d\vartheta \tag{20}$$

ϑ is the angle between the radius vector and the direction of sedimentation. The earlier expressions[7] for v_r and v_ϑ yield with eq 20

$$\langle v_r \rangle_\perp = (k/4\pi\eta) \ln (2r/d) \qquad \text{uncharged rods} \tag{21}$$

$$\langle v_r \rangle_\perp = (k/4\pi\eta)\left[\ln (2r/d) - \int_{\kappa a}^{\kappa r} \xi\, ds\right] \qquad \text{charged rods} \tag{22}$$

The integrand ξ in eq 22 is a complicated function of the double-layer potential; k is the sedimentation force per unit length rod. Outside the double layer eq 22 takes the form

$$\langle v_r \rangle_\perp = (k/4\pi\eta)[\ln (2r/d) - g], \quad r \gg 1/\kappa \qquad \text{charged rod} \tag{23}$$

where the function g, denoted f in ref 7, is

$$g = \int_{\kappa a}^{\infty} \xi\, ds \tag{24}$$

In practice, we deal with randomly oriented rods. For further averaging we need the velocity $v_{r\parallel}$ of the liquid when it flows past an uncharged rod in parallel motion. This is well approximated by a stationary cylinder of diameter d inside a coaxial cylinder of diameter $D \gg d$. When the outer cylinder moves with velocity u along the common axis, the liquid occupying the space between the concentric surfaces moves at distance r from the axis with velocity[23]

$$v_{r\parallel} = u\frac{\ln (2r/d)}{\ln (d/D)} \tag{25}$$

With the friction force on the inner cylinder, k per unit length, given by

$$k = \pi d\eta(dv/dr)_{r=d/2} = (2\pi\eta u)/\ln (d/D) \tag{26}$$

eq 25 becomes

$$v_{r\parallel} = (k/2\pi\eta) \ln (2r/d) \tag{27}$$

We neglect end effects of the rod and, hence, the relaxation effect on its lengthwise sedimentation. With the average for random orientation

$$\langle v_r \rangle = (2\langle v_r \rangle_\perp + v_{r\parallel})/3 \tag{28}$$

we find for randomly oriented rods from eq 21, 22, and 27

$$\langle v_r \rangle = (k/3\pi\eta) \ln (2r/d) \qquad \text{uncharged} \tag{29}$$

$$\langle v_r \rangle = (k/3\pi\eta)[\ln (2r/d) - g/2], \quad r \gg 1/\kappa \qquad \text{charged} \tag{30}$$

As for the sphere, the net relaxation force on the charged rod vanishes, so that the sedimentation force k is the same in eq 29 and 30. We now replace the charged rod by an uncharged rod of diameter d_{rel} such that the outer flow field in eq 30 remains the same. This gives the relation

$$\ln (2r/d) - g/2 = \ln (2r/d_{rel}) \tag{31}$$

or

$$d_{rel} = d \exp(g/2) \tag{32}$$

The diameter d_{rel} was evaluated for DNA in NaCl solutions from available data[7] on the relaxation correction g for a charge of 0.65 electron per DNA phosphate. Results are shown in Table II. It is noted that d_{rel} is always smaller than the statistical exclusion diameter d_B in Table I. So there is no inconsistency in using d_{rel} for the chain diameter in all probable coil conformations.

In a sedimentation or a viscosity experiment each chain segment moves in a liquid velocity field determined by external conditions and by the contributions of all other chain segments. The orientation of each segment with respect to this flow field is random, by virtue of the chain statistics. For this reason the averaging method of eq 28 is appropriate under all conditions and the renormalization of the chain diameter by eq 32 is valid in (weak field) hydrodynamic experiments that do not perturb the chain orientation significantly such as sedimentation, diffusion, and viscosity.

4. Sedimentation

The sedimentation of polyelectrolytes involves four different charge effects: the repulsion of salt, the influence of the coil expansion on the drainage, the short-range effect of the asymmetry of the double layer on the local friction of the chain, and the modification of the coil velocity by the long-range field of the relaxation dipoles. In this

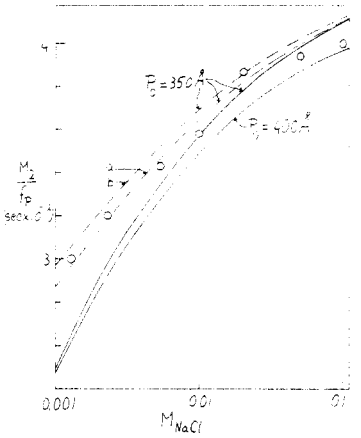

Figure 7. Inverse friction factor M_2/f_p of native T7 DNA in NaCl solutions. Circles from experiments[1,26] with eq 35.[27] Solid curves from eq 42 for two values of persistence length as indicated. Curve a, from eq 42 with $\Delta s^0 = 0$; curve b, from eq 42 with $\Delta s^0 = 0$ and $d_{rel} = d = 24$ Å.

section we introduce each effect separately.

Eisenberg has shown that the limiting sedimentation coefficient, s^0, of a polyelectrolyte in an aqueous salt solution is given by[24]

$$s^0 = \frac{M_2 D^0}{RT}\left(\frac{\partial \rho}{\partial c_2}\right)_{P,\mu_3} \tag{33}$$

where D^0 is the diffusion factor and c_2 is the concentration in g/mL of the polyelectrolyte (component 2) with molecular weight M_2, and ρ is the density of the salt solution. The density increment at constant chemical potential of the salt (component 3) takes into account the negative adsorption of the salt, Γ grams of salt per gram of polyelectrolyte. In terms of the partial specific volumes $\bar{v}_2{}^0$ and $\bar{v}_3$ we have[25] for $c_2 \to 0$

$$\left(\frac{\partial \rho}{\partial c_2}\right)_{P,\mu_3} = (1 - \bar{v}_2{}^0\rho) + \Gamma(1 - \bar{v}_3\rho) \tag{34}$$

For $\Gamma = 0$ the familiar equation for the sedimentation in two-component systems is recovered from eq 33 and 34.

Equation 33 rests on the assumption that during sedimentation of the polyelectrolyte the salt is always in equilibrium. In most experiments this assumption, μ_3 = constant, is probably a good approximation. In a more recent model treatment Eisenberg[26] has connected the sedimentation coefficient of polyelectrolytes with ionic friction factors. For $c_2 = 0$ the limiting result is

$$s^0 = \frac{M_2}{f_p}\left(\frac{\partial \rho}{\partial c_2}\right)_{P,\mu_3} \tag{35}$$

where f_p is the molar friction factor of the polyion. The independence of s^0 from the friction factor of the counterions is not self-evident. This point will be discussed later.

Rinehart and Hearst[27] have used eq 35 to recalculate M_2/f_p from the sedimentation measurements of T7 DNA by Rosenberg and Studier[1] and density data by Cohen and Eisenberg.[25] The results, given by the circles in Figure 7, will be compared with the theoretical results of M_2/f_p developed below.

Yamakawa and Fujii[3] have derived the translational friction factor f of uncharged, stiff chains without excluded volume by an application of the Oseen–Burgers procedure of hydrodynamics to wormlike cylinder models. For polymers with contour length L, persistence length P, and hydrodynamic chain diameter d, the theory predicts

$$3\pi\eta_0 L/f = \sum_{i=1}^{5} A_i (L/2P)^{1-i/2} \tag{36}$$

where η_0 is the solvent viscosity and the coefficients A_i are given as functions of $d/2P$. Several modifications are necessary to correct eq 36 for preaveraging approximations and to allow for relaxation and excluded volume effects in T7 DNA.

The derivation[3] of eq 36 follows Kirkwood and Riseman[28] in applying the preaveraged Oseen tensor to evaluate the hydrodynamic interactions between chain segments in the average polymer configuration. From a Monte Carlo study Zimm[5] has concluded that these preaveraging approximations yield sedimentation coefficients that are about 13% too high. Accordingly, we shall divide results of eq 36 by a factor 1.13.

We now turn to the charge effects. As explained in section 3, the relaxation effect is adsorbed in the renormalized hydrodynamic diameter d_{rel} of the chain. The data on α^3 in Table I show that the excluded volume effect may increase the size of T7 DNA coils considerably. We accommodate this increase by modifying the chain statistics as follows. The chain is stiffened such that with elimination of the excluded volume the average coil size remains unchanged. To this end we assume $d_B = 0$ in eq 8 and replace P by an effective persistence length $P_{eff} = 3s^2/L$, where s is the radius of gyration of the coil with excluded volume. We see from eq 9 that $P_{eff} = (P_0 + P_{el})\alpha^2$. In summary, we model T7 DNA as an uncharged wormlike cylinder without excluded volume, with contour length L, persistence length P_{eff}, and hydrodynamic diameter d_{rel}. With these changes eq 36 becomes

$$3\pi\eta_0 L/f = (1/1.13)\sum_{i=1}^{5} A_i (L/2P_{eff})^{1-i/2} \tag{37}$$

where the coefficients A_i are now functions of $d/2P = d_{rel}/2P_{eff}$.

Results for T7 DNA are given in Table II, based on $P_0 = 400$ Å and the s values for the uniform spherical model, eq 8a in Table I. P_{eff} is found to be 12–57% greater than the persistence length $P = P_0 + P_{el}$ in Table I. Most of the change of the factor $3\pi\eta_0 L/f$ with ionic strength derives from the variation of P_{eff}, that is, from the coil expansion. The contribution of the relaxation effect, the change from d to d_{rel} in eq 37, is maximal 3.5%.

It remains to introduce the second part of the relaxation effect, typical for polyelectrolyte coils, due to the extra electrostatic field produced by the asymmetric double layer. As shown schematically in Figure 4, during sedimentation each charged segment with its ionic atmosphere acts as a dipole. The dipole strength is proportional to the local polarization; it depends on the orientation of the segment and on the local liquid velocity. Each charged segment moves in the dipole field of all other segments. The resulting reduction of the segment velocity is proportional to the electrophoretic mobility of the polyion. We evaluate this second part of the relaxation effect with a simple approximate model. We assume that the coil is fully drained, that it has spherical symmetry, and that the relaxation polarization is continuous and uniform in the sphere, as pictured in Figure 8a. This approximate model is expected to give an upper boundary of the correction.

As explained in texts on dielectric theory, the field inside a uniformly polarized body depends on the shape of the body. If P' is the volume polarization, the internal field of the sphere of Figure 8a is $4\pi P'/3$, while inside a polarized slab, Figure 8b, the polarization field is $4\pi P'$. The

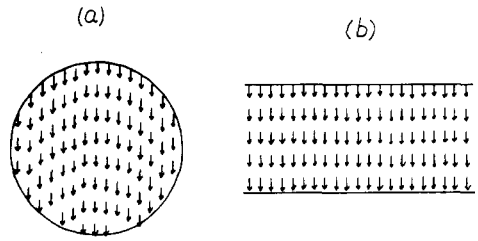

Figure 8. Uniformly polarized sphere (a) and slab (b).

slab has the symmetry of the usual transport cells and allows us to derive the sedimentation polarization P' from electrophoretic experiments. Consider a salt solution which is uniformly filled with polyelectrolyte, that is, with $n = 1/V$ coils per unit volume, when V is the volume of one coil. When subjected to sedimentation in a field g_{sed} the solution becomes uniformly polarized. If no current passes through the cell, $i = 0$, the result is a sedimentation potential E_{sed} and the polarization field is given by

$$4\pi P' = (E_{sed}/g_{sed})_{i=0} \tag{38}$$

de Groot et al.[29] have connected the sedimentation potential with electrophoresis through the thermodynamics of irreversible processes. In the present notation the relation is

$$\left(\frac{E_{sed}}{g_{sed}}\right)_{i=0} = -\frac{nM_2}{\kappa_{spec}}\left(\frac{\partial\rho}{\partial c_2}\right)_{P,\mu_3}\left(\frac{u}{E}\right)_{g_{sed}=0} \tag{39}$$

With eq 38 and 39 the volume polarization P' can be expressed in terms of the specific conductance of the solution, κ_{spec}, and the electrophoretic mobility, u/E, measured under the usual experimental conditions when sedimentation is absent.

We now return to the single polyelectrolyte sphere sedimenting in unit field. The polarization field inside the sphere, $4\pi P'/3$ gives an electrophoretic contribution to the velocity of the sphere which follows from eq 38 and 39

$$\Delta s^0 = \frac{4\pi P'}{3}\frac{u}{E} = -\frac{nM_2}{3\kappa_{spec}}\left(\frac{\partial\rho}{\partial c_2}\right)_{P,\mu_3}\left(\frac{u}{E}\right)^2 \tag{40}$$

and with eq 35 the relative change of s^0 becomes

$$\frac{\Delta s^0}{s^0} = -\frac{nf_p}{3\kappa_{spec}}\left(\frac{u}{E}\right)^2 \tag{41}$$

The theoretical correction $\Delta s^0/s^0$ is applied to the friction factor of the coil. With eq 37 this leads to the final theoretical expression

$$\frac{M_2}{f_p} = \frac{M_2}{3\pi\eta_0 L}\frac{3\pi\eta_0 L}{f}\left(1 + \frac{\Delta s^0}{s^0}\right) \tag{42}$$

In eq 41 the coil volume $1/n = V$ is given by eq 11. For κ_{spec} at $c_2 = 0$ data on NaCl solutions are available in the literature. The friction factor f_p is obtained from the experimental data on M_2/f_p in Figure 7. Electrophoretic mobilities are taken from moving-boundary experiments[30] at 1.3 °C. Values of u/E, corrected to 20 °C for the viscosity change of water, are given in Table II, along with other factors in eq 42.

In Figure 7 results for M_2/f_p are plotted vs. the ionic strength and compared with experiments. The full curves were obtained from eq 42, for chains with intrinsic persistence length $P_0 = 350$ and 400 Å. The dashed curves for $P_0 = 350$ Å show the influence of the relaxation effect. Curve a was computed from eq 42 with $\Delta s^0 = 0$; curve b was also computed from eq 42 with $\Delta s^0 = 0$ and, in addition, $d_{rel} = d = 24$ Å. So the difference between curves a and b is only the short-range relaxation friction, which contributes less than 3% to the total friction. The only adjustable parameter in the theory is the intrinsic persistence length P_0. Remembering that the present theory overestimates $\Delta s^0/s^0$, the comparison with the experiments in Figure 7 suggests $P_0 \approx 350$ Å as the best value.

5. Intrinsic Viscosity

The intrinsic viscosity of uncharged, linear polymers may be expressed in terms of the radius of gyration s and the polymer weight M_2 by[31]

$$[\eta] = \Phi(6^{1/2}s)^3/M_2 \tag{43}$$

where the factor Φ depends on the hydrodynamic interactions between the polymer segments. In a sequel to the friction theory[3] Yamakawa and Fujii have derived Φ for their model of wormlike chains without excluded volume.[4] Their result for long polymers is

$$\Phi = \Phi_\infty[1 - \sum_{i=1}^{4} C_i(L/2P)^{-i/2}]^{-1} \tag{44}$$

with $\Phi_\infty = 2.87 \times 10^{23}$ and the coefficients C_i given as polynomials in $d/2P$.

Our modifications of eq 44 for application to T7 DNA are similar to those of eq 36 for the friction. To correct for the preaveraging approximations we take for Φ_∞ the value 2.51×10^{23} reported by Zimm in this Monte Carlo study.[5] To introduce excluded volume effects and relaxation friction we take P_{eff} for P and d_{rel} for d so that eq 44 becomes

$$\Phi = 2.51 \times 10^{23}[1 - \sum_{i=1}^{4} C_i(L/2P_{eff})^{-1/2}]^{-1} \tag{45}$$

with the coefficients C_i now as functions of $d_{rel}/2P_{eff}$.

We now consider the change of $[\eta]$ due to the long-range field of the relaxation dipoles. We assume the same model as in sedimentation, a completely drained, uniformly polarizable, uniformly charged sphere. This sphere is in a uniformly sheared salt solution. The volume polarization P' of the sphere is not uniform as in sedimentation, since it is proportional to the local liquid velocity relative to the segments of the sphere. The segment velocity, a rotation, produces a circular component of P'. Now, the line integral of an electrostatic field along any closed circular path must vanish. Hence, a rotation component of P' can exert neither force nor torque on the sphere. The residue of P', proportional to the external shear gradient, is decomposed in a strain and a rotation field, as is usual in fluid dynamics. Inspection shows that the total force and torque due to the strain field, of the form ($P'_x = y$, $P'_y = x$, $P'_z = 0$), vanish by symmetry. The rotation field cannot contribute either and is, furthermore, opposed by the field due to the rotation of the sphere. In summary, the long-range effect of the relaxation field on $[\eta]$ vanishes as a first approximation.

Values of Φ for T7 DNA in NaCl solutions are presented in the last column of Table II, calculated from eq 45 assuming $P_0 = 400$ Å. The intrinsic viscosity $[\eta]$ can now be obtained from eq 43 with the s values of Table I, eq 8a for $P_0 = 400$ Å. The results for $[\eta]$ are represented by the lower solid curve in Figure 9. The variation of Φ partly compensates for the large change in coil size, proportional to s^3. Nevertheless, the theory predicts a more than threefold change of $[\eta]$ in the range of ionic strength under study.

The dashed curve in Figure 9 is also for $P_0 = 400$ Å, but omitting the relaxation effect, that is, computed with chain

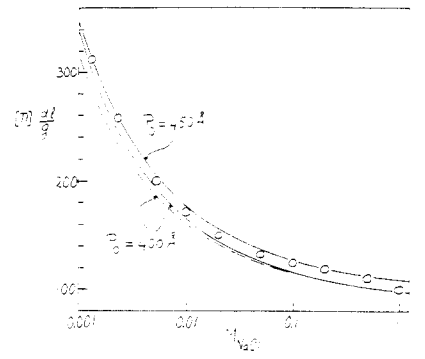

Figure 9. Intrinsic viscosity of native T7 DNA in NaCl solutions. Circles from experiments by Rosenberg and Studier.[1] Solid curves from eq 43 and 45 with intrinsic persistence length P_0 as indicated. Dashed curve, without relaxation effect, $d_{rel} = d = 24$ Å in eq 45.

diameter $d_{rel} = d = 24$ Å in all cases. The small difference with the lower solid curve shows the relatively minor influence of the relaxation effect on $[\eta]$, not unexpected in view of the earlier findings for sedimentation.

The difference between the two solid curves in Figure 9 shows that stiffening the chain, from $P_0 = 400$ Å to P_0 450 Å, causes $[\eta]$ to increase significantly, due to the enlarged coil; compare Figure 3. The circles in Figure 9 are the experimental values by Rosenberg and Studier.[1] These points exhibit the expected trend with ionic strength; comparison with the solid lines suggests an intrinsic persistence length of $P_0 \approx 425$ Å for native DNA.

6. Discussion and Comments

The salt effects on the transport properties measured for T7 DNA agree well with the predictions, in particular for the viscosity in Figure 9, and considering that the solid curves for the sedimentation in Figure 7 overestimate the effects of the long-range relaxation field in Δs^0.

The theoretical curves in Figures 7 and 9 are for the uniform spherical coil model. The other models under consideration, Gaussian sphere and uniform ellipsoidal coil, predict for the same P_0 between 3.3% and 7.2% lower values of $[\eta]$ and from 1.1% to 2.1% higher values of M_2/f_p. These small differences between the three models are of doubtful significance.

The two independent estimates of the intrinsic persistence length are in the same range, but their difference is probably significant, $P_0 \approx 350$ Å from sedimentation and $P_0 \approx 425$ Å from viscosity. The main reason for the difference might be that the transport theory[3-5] is for random flight chains, while T7 DNA coils have a sizable excluded volume effect that required a change in the statistical segment distribution by the introduction of P_{eff}. It would be interesting to perform Monte Carlo computations on DNA chains with excluded volume and relaxation effects. In particular, the effects of the long-range dipole field could be studied more rigorously.

There are no suitable data in the literature to test the predictions of coil size in Figure 3. The reason is that extreme dilution would be required for light scattering experiments. The range of s values in Figure 3 from 5000 to 8000 Å corresponds to coils with a DNA concentration from 23.4 to 5.7 μg/mL, assuming the uniform spherical coil model. In solutions with a higher concentration of T7 DNA neighboring coils must overlap. Therefore, light scattering experiments should be carried out well below the above DNA concentrations to avoid coil overlap and unreliable extrapolation to infinite dilution. However, at such low concentrations the intensity of the light scattered by the DNA is so small that accurate determinations become difficult.

The contribution of the counterions to the friction of polyelectrolytes calls for additional comments. In eq 35 the driving force is $M_2(\partial\rho/\partial c_2)_{P,\mu_3}$; f_p is the friction of only the polyion itself, excluding any contribution of the counterions. In the derivation of eq 35 Eisenberg[26] assumed overall electroneutrality of the solution and coupling between polyion and small ions through the sedimentation potential. In the extrapolation $c_2 \to 0$ for obtaining s^0 the sedimentation potential vanishes and, hence, there is no coupling left between polyion and small ions. Therefore, eq 35 is consistent with Eisenberg's assumption, although it is not necessarily a good approximation.

In general, electroneutrality is maintained not only on a macroscale in the solution, as implied in Eisenberg's treatment, but also on a microscale between a polyion and its ionic atmosphere. To some extent the polyion pulls counterions with it in sedimentation, some degree of coupling between polyion and counterions being maintained even without a macroscopic sedimentation potential. Actually, the ionic atmosphere around the moving polyion is continually restored by electrostatic and diffusion forces. Both forces arise from the asymmetric perturbation of the equilibrium double layer during sedimentation, as illustrated for spherical colloid particles in Figures 5 and 6 of ref 21. The ion diffusion forces, arising from the mutual diffusion of water and small ions, do not add to the friction of the polyion; only the electric "relaxation forces" have to be counted. This is consistent with our relaxation treatment in section 3, as may be argued as follows.

According to the law action = reaction the electric relaxation force on the countercharge is balanced by an electrical force on the charge rod, due to its asymmetric atmosphere. This is an extra force to be counted in the balance of forces on the rod in steady motion. As stated in section 3, the electrical relaxation force on the rod is exactly compensated by the hydrodynamic drag forces on the surface of the rod from the extra flow illustrated in Figure 5. This is the flow giving the relaxation correction g in eq 24, accounted for in the renormalized diameter of the rod in eq 32. In this way the short-range relaxation correction of the friction of the polyion originates from the short-range relaxation coupling with the countercharge.

One of our main conclusions is that the ionic relaxation effect on polyelectrolyte friction is rather small. This does not agree with a recent theory by Schurr.[6] He has used a fluctuating-force approach to derive the friction of a charged gel sphere model of polyelectrolytes in symmetric salt solutions in which all small ions have the same friction factor. The results for the relaxation effect, termed electrolyte friction by Schurr, may be compared with those by Booth[32] on a sedimenting, charged sphere. The ratio of the charge effect on the friction as calculated by Schurr, Δf_S, to that by Booth, Δf_B, is only a function of κa, the radius of the colloid sphere in units of the Debye length $1/\kappa$. For $\kappa a = 1.9$, 3.2, and 5.9, we find $\Delta f_S/\Delta f_B = 19$, 31, and 74, respectively. These ratios illustrate the large difference between the two theories. It is noted that Booth[32] started from a well-established set of electrohydrodynamic equations and his analytical results have been confirmed by Stigter's numerical treatment[21] of the same problem.

Although ultracentrifugal sedimentation may be an outdated experimental method, ionic relaxation effects, or electrolyte friction, appear also in current dynamic light scattering methods for measuring diffusion and electrophoresis. We are in an interesting phase of development. More experimental data will be produced, with many difficult problems in interpretation. Fluctuation theory

should give the same answers as fluid dynamics, at least on a colloidal scale. It is important that the large difference between Schurr's fluctuating-force treatment[6] and the older hydrodynamic work[21,32] be resolved.

Acknowledgment. I am grateful to Professor D. W. Fuerstenau for his hospitality at the University of California, Berkeley, and for computer funds to finish this project. Correspondence with Professor J. M. Schurr about his fluctuating-force treatment stimulated the present study.

Registry No. NaCl, 7647-14-5.

References and Notes

(1) Rosenberg, A. H.; Studier, F. W. *Biopolymers* **1969**, *7*, 765.
(2) Rinehart, F. P.; Hearst, J. E. *Arch. Biochem. Biophys.* **1972**, *152*, 712.
(3) Yamakawa, H.; Fujii, M. *Macromolecules* **1973**, *6*, 407.
(4) Yamakawa, H.; Fujii, M. *Macromolecules* **1974**, *7*, 128.
(5) Zimm, B. H. *Macromolecules* **1980**, *13*, 592.
(6) Schurr, J. M. *Chem. Phys.* **1980**, *45*, 119.
(7) Stigter, D. *J. Phys. Chem.* **1982**, *86*, 3553. The relaxation correction f is denoted g in the present paper.
(8) Le Bret, M. *C. R. Hebd. Seances Acad. Sci.* **1981**, *292*, 291.
(9) Fixman, M. *J. Chem. Phys.* **1982**, *76*, 6346.
(10) Stigter, D. *Macromolecules* **1982**, *15*, 635.
(11) (a) Hermans, J. J.; Overbeek, J. Th. G. *Recl. Trav. Chim. Pays-Bas* **1948**, *67*, 761. (b) Dunn, J. J.; Studier, F. W. *J. Mol. Biol.* **1983**, *166*, 477.
(12) Stigter, D. *Biopolymers* **1977**, *16*, 1435.
(13) Debye, P.; Bueche, F. *J. Chem. Phys.* **1952**, *20*, 1337.
(14) Kurata, M.; Stockmayer, W. H.; Roig, A. *J. Chem. Phys.* **1960**, *33*, 151.
(15) Schellman, J. A.; Stigter, D. *Biopolymers* **1977**, *16*, 1415.
(16) Flory, P. J. *J. Chem. Phys.* **1949**, *17*, 303.
(17) Flory, P. J.; Fox, T. G. *J. Am. Chem. Soc.* **1951**, *73*, 1904.
(18) Peterlin, A. *J. Chem. Phys.* **1955**, *23*, 2464.
(19) Douthart, R. J.; Bloomfield, V. A. *Biopolymers* **1968**, *6*, 1297.
(20) Cotter, M. A.; Martire, D. E. *J. Chem. Phys.* **1970**, *52*, 1909.
(21) Stigter, D. *J. Phys. Chem.* **1980**, *84*, 2758.
(22) Wiersema, P. H. Thesis, Utrecht, 1964.
(23) Landau, L. D.; Lifshitz, E. M. "Fluid Mechanics"; Pergamon Press: New York, 1959; p 58.
(24) Eisenberg, H. *J. Chem. Phys.* **1962**, *36*, 1837.
(25) Cohen, G.; Eisenberg, H. *Biopolymers* **1968**, *6*, 1077.
(26) Eisenberg, H. *Biophys. Chem.* **1976**, *5*, 243.
(27) Rinehart, F. P.; Hearst, J. E. *Biopolymers* **1972**, *11*, 1985.
(28) Kirkwood, J. G.; Riseman, J. *J. Chem. Phys.* **1948**, *16*, 565.
(29) de Groot, S. R.; Mazur, P.; Overbeek, J. Th. G. *J. Chem. Phys.* **1952**, *20*, 1825.
(30) Ross, P. D.; Scruggs, R. L. *Biopolymers* **1964**, *2*, 231. Ross, P. D. *Biopolymers* **1964**, *2*, 9.
(31) Flory, P. J. "Principles of Polymer Chemistry"; Cornell University Press: Ithaca, NY, 1953; pp 609–611.
(32) Booth, F. *J. Chem. Phys.* **1954**, *22*, 1956.